Uptake and toxicity of different nanoparticles towards a tough bacterium: *Deinococcus radiodurans*

Ragini Singh and Sanjay Singh*

Biological & Life Sciences, School of Arts & Sciences, Central Campus, Ahmedabad University, Navrangpura, Ahmedabad-380009, Gujarat, India.

*Corresponding author

DOI: 10.5185/amlett.2018.2064
www.vbripress.com/aml

Abstract

Nanomaterials (NMs) have found extensive commercial use in industries, healthcare and household applications however, their ecotoxicological effects remain elusive. Since, microbial communities play beneficial role in ecosystem like element cycling, bioremediation, nitrogen fixation, etc., effect of NMs over beneficial microbe's physiology and viability remains to be studied in detail. Some beneficial microbe communities are severely affected by the release of NMs in the environment. *Deinococcus radiodurans* is known for its tolerance to oxidative stress caused due to irradiation. In this study, we have used metal, metal oxides, quantum dots (QDs) and carbon based NMs to assess their effect on the cell viability, uptake and ROS generation in *D. radiodurans* cells. The present study demonstrates in real-time by flow cytometry the internalization of different metal, metal oxide, QDs and carbon based NMs in *D. radiodurans.* Results show that all the tested NMs are significantly internalized in to the bacterial cells however, carbon based NMs exhibited highest internalization. Toxicity studies revealed that AgNPs exhibited maximum toxicity and reactive oxygen species (ROS) generation followed by QDs, CuO NPs and GO but, AuNPs and TiO_2 NPs shows no toxic response in bacterial cells. The oxidative stress and uptake studies will provide insight about the mechanism of oxidative stress tolerance of *D. radiodurans.*

Keywords: *Deinococcus radiodurans*, flow cytometry, nanoparticles uptake, metal, metal oxide, quantum dots, carbon based nanomaterials.

Introduction

Recent progress in the area of nanoscience and nanotechnology has led to the use of nanomaterials (NMs) more efficiently in industrial and biomedical applications. The unique optical, mechanical, electrical and magnetic properties of NMs are reported due to high surface to volume ratio and surface reactivity which are dependent on the shape, size and composition of material [1, 2]. Although several beneficial biomedical applications of NMs are recently reported, however, the harmful impact of NMs on human health and environment has become a bottleneck for the implementation of real potential of nanotechnology. European Union and United states legislative bodies have focused their activities to assess the health and environmental risks of NMs [1]. Risk assessment of NMs in context of environment require the information about their fate after release i.e. reactivity, mobility, persistence in environment, and also their effect on living organisms [3].

Many beneficial microbial communities play important role in ecosystem such as bioremediation, element cycling and nitrogen fixation for plant growth [4-6]. These microbes can be severely affected by the presence of nanoparticles (NPs) in the environment [7]. Exact mechanism of antimicrobial properties of NPs are still unknown, but it may vary for different bacteria. NPs may get attach to the bacterial membrane by electrostatic interaction, and disrupt the membrane integrity [8]. Administration of NPs usually prompts the free radical formation inside the cells and cause oxidative stress [9, 10]. Physicochemical properties of NPs and type of bacteria are the two main factors that govern the antibacterial properties of NPs [11]. It is reported that slow-growing bacteria are less prone to antibiotics and NMs than fast-growing bacteria [12, 13].

Silver NPs (AgNPs) are reported to be extremely toxic for the bacterial cells, its toxicity mechanism was thought to be due to the disruption of membrane and irreversible binding of Ag ions with essential biomolecules of bacterial strains.[11]. In *E.coli* cells, it is reported that AgNPs target the bacterial membrane which leads to loss of proton motive force [14]. AgNPs are also shown to be adsorbed on bacterial membrane. This causes more toxicity in *Pseudomonas aeruginosa* and different bacterial species at acidic pH (5) than alkaline pH (9) due to electrostatic force of attraction [11]. Chatterjee et al. reported that gold NPs (AuNPs) are non-toxic to the bacterial cells and have no significant impact on their growth [15]. Similar, result was reported

by Connor *et al*., AuNPs are internalized into the human cells but do not cause any acute toxicity [16]. Eco toxicity of metal oxide NPs such as Copper oxide (CuO) and Titanium dioxide (TiO_2) NPs has been studied in several bacterial and yeast species [17, 18]. Results revealed that TiO_2 NPs are non-toxic to the bacterial and yeast cells whereas, CuO NPs were found to be highly toxic. Toxicity of CuO NPs were thought to be due the bioavailability of solubilized Cu ions in the growth medium [17, 18]. Monras et al. [19] reported the toxicity of CdTe quantum dots (QDs) via oxidative stress, disruption of membrane integrity and reactive oxygen species (ROS) generation. Red QDs were reported to be more toxic than green QDs in *E.coli* cells due to more cadmium ions and also make it more sensitive towards polymyxin B. On exposure of QDs, superoxide dismutase genes (SOD) was up-regulated in *Pseudomonas stutzeri* which corresponds to production of ROS inside cells [19]. Carbon based NMs possesses the antibacterial mechanism due to its interaction with bacterial cell surface, affecting their metabolic processes and morphology. It was reported that due to smaller diameter single wall carbon nanotubes (SWNTs) can penetrate the bacterial cells more easily in comparison to multi wall carbon nanotubes (MWNTs) in *E.coli*, hence causes more toxic effect [20]. They form cell-CNTs aggregates and induces cell wall damage which causes release of bacterial DNA content. Graphene oxides (GO) were shown to have inhibitory effect on the growth of *E. coli* cells. Their sharp edges damage the cell membrane and cause RNA efflux in both gram positive and gram negative bacteria [20]. Antibacterial activity of fullerenes were also reported against *E. coli*, *Salmonella* and *Streptococcus* species, which was thought to be due to the inhibition of energy metabolism [20].

D. radiodurans are known for its extraordinary resistance against gamma radiation, desiccation and mitomycin C [21]. They also display remarkable oxidative stress resistance due to the presence of highly efficient enzymatic and non-enzymatic small molecule antioxidants [21, 22]. Their robustness is derived by protection of protein from oxidative damage and strong DNA repair mechanism [21] and manganese complex [23]. They are gram positive bacteria, but due to their lipid composition and multilayered structure of cell membrane, they reminiscent the gram negative bacteria [21, 24, 25]. So far, no comprehensive studies are made to illustrate the impact of NMs on the *D. radiodurans*. There are several reports illustrating the effects of NMs on the viability and mediated oxidative stress of several grams positive and gram negative bacterial strains. However, it will be interesting to explore the cell viability and oxidative stress generation in bacterial strain capable to withstand the effects of radiation and free radicals. *D. radiodurans* was chosen in this study as a model organism exhibiting strong resistance to oxidative stress generated due to radiation exposure, however, we exposed this strain to various NMs and studied the effects on viability and oxidative stress. In this study we have included various NMs i.e. metallic (AuNPs and AgNPs), metal oxides (CuO and TiO_2 NPs), Cadmium Telluride (CdTe) QDs and Carbon based NMs (GO, SWCNTs and fullerenes).

Experimental section

Materials

Gold [752584]; silver nanoparticle dispersion [730785]; copper (II) oxide [CAS: 1317-38-0, 544868]; titanium (IV) oxide, mixture of rutile and anatase [CAS: 13463-67-7, 700347]; graphene oxide [796034]; carbon nanotube, single walled [CAS: 308068-56-6, 704121] and fullerenes-C_{60} [CAS: 99685-96-8, 379646] and 2'-7'-dichlorodihydrofluorescein diacetate (DCFH-DA) dye were purchased from Sigma Aldrich (St. Louis, MO USA). CdTe QDs [RN -PL -QDN-510] were obtained from Reinste, India. Phosphate Buffer Saline (PBS) and 3-(4,5-dimethylthiazol-2-yl)-2,5-diphenyl tetrazolium bromide (MTT) were obtained from Himedia, India.

NPs suspension

Stock of NPs suspension were prepared by suspending 1.5 mg of NMs in 10 mL of Milli Q by sonicating at 30W for 10 min (pulse of 2 min 'on' and 1 min 'off'), when needed.

Culture of D. radiodurans

D. radiodurans R1 strain BAA 816 culture (5 mL) was grown overnight at 32°C in TGY media (1% tryptone, 0.1% glucose and 0.5% yeast extract) by shaking at 150 rpm [22]. Bacterial growth was monitored by measuring the turbidity of culture at 600 nm using spectrophotometer. Overnight grown culture was then re-inoculated into fresh TGY media (at A_{600}=0.1) and allowed to grow up in log phase (A_{600}=0.65±0.05) for further experiment.

Exposure of D. radiodurans to NMs

D. radiodurans cells (~0.6×10^8 CFU/mL) were pelleted down by centrifugation at 4000 rpm for 5 min. Cells pellet was washed twice with PBS. Further, cells were exposed to different concentrations of metal [AgNPs and AuNPs] (1, 5, 10, 15 and 20 µg/mL), metal oxide [CuO and TiO_2], CdTe QDs and carbon based NMs [CNTs, GO and fullerenes] (5, 10, 20, 40 and 80 µg/mL) in a total volume of 3 mL for 3 hrs at 32°C in PBS.

Preparation of samples for flow cytometry

After 3 hrs of exposure to NMs, bacterial cells (~0.6×10^8 CFU/mL) were diluted in 1 mL PBS and 10,000 cells were acquired by flow cytometer (FACS Calibur, BD Biosciences, CA) in each of the control (without any NPs exposure) and treated sample. Side scattering intensity (SSC) were recorded in each case. Forward scatter (FSC), SSC and FITC (green fluorescence) were set to logarithmic scale. NPs without bacterial cells were run in parallel for each sample to minimize any interference.

Preparation of sample for scanning electron microscope

After 3 hrs exposure to carbon based NMs (GO and CNTs) at 80 µg/mL concentration, control and treated bacterial cells (~ 0.6 x 10^8 CFU/mL) were gently washed with PBS for 3 times. Further, cell pellet was fixed with 1 mL of 2.5% glutaraldehyde for 30 min at 4°C. After fixation, a dehydration series was performed using different ethanol concentration i.e. 15, 30, 50, 70% of ethanol in water each for 20 min and at last cells were fixed in 100% ethanol 3 times each for 20 min. Dehydrated cells were kept overnight for complete drying and thereafter samples were analyzed using SEM (Jeol JSM 6010 LA).

Preparation of sample for transmission electron microscope

After 3 hrs exposure to carbon based NMs (GO and CNTs) at 80 µg/mL concentration, control and treated bacterial cells suspension (~ 0.6 x 10^8 CFU/mL) were fixed with 1 mL of 2.5% glutaraldehyde at 4°C for 30 min. Cells were pelleted down and washed with 0.1M sodium cachodylate buffer followed by fixation in 100 µL of 2% osmium tetraoxide for 2 hrs at 4°C. Fixed pellet were washed with sodium cachodylate buffer and undergo dehydration series through different grades of ethanol i.e. 30–70% of ethanol in water, each for 20 min and at last dehydrated in 100% ethanol 3 times for 20 min. Sample was then embedded in araldite resin and kept at 60°C for 72 hrs. Further, ultrathin sections were prepared using ultra microtome (Leica UC7) and the grids were examined under a TEM (Jeol JEM1400 Plus) at an accelerating voltage of 100 kV.

Cell viability assay

MTT reduction by cells corresponds to its viability and was determined as described below. After 3 hrs exposure to NMs at different concentrations, 100 µL of control and treated bacterial cells (~0.6 × 10^8 CFU/mL) were transferred to 96 well plates (per well). 10 µL of MTT dye (5 mg/mL in PBS) were added into each well and then incubated for 2-3 hrs at 37°C. Formazan crystals formed, were dissolved in DMSO (100 µL), and incubated at 37°C for 30 min. Absorbance was measured at 570 nm using multichannel plate reader (Biotek, Synergt HT spectrophotometer). Viability was calculated by the formula given below: % Viable cells = ($O.D._{570}$ of NMs treated cells/$O.D._{570}$ of control cells) × 100

Determination of reactive oxygen species

D. radiodurans cells were treated with different concentrations of NMs for 3 hrs. 100 µL of control and treated bacterial cells (~ 0.6 x 10^8 CFU/mL) were transferred to 96 well black bottom plate (per well) and incubated with 100 µL DCFDA dye (20 µM) for 30 min at 37°C. Fluorescence intensity was measured at an excitation and emission wavelength of 485 and 528 nm respectively using a multiwell plate reader (Biotek, Synergy HT spectrophotometer)intensity was measured at an excitation and emission wavelength of 485 and 528 nm respectively using a multiwell plate reader (Biotek, Synergy HT spectrophotometer).

Results and discussion

NPs can be internalized into the bacterial cells through different mechanism like non-specific diffusion, non-specific membrane damage and specific uptake (silCBA gene transportation system, through porins) but the method of quantitative estimation of NMs uptake in bacterial cells is still unidentified. Few recent studies demonstrated that the cellular uptake of the ZnO NPs in *E. coli* and *S. typhimurium* cells can be achieved by TEM [26-28] and flow cytometry [29]. NPs internalization in human cells can also be detected by flow cytometry based on increase in granularity [30, 31].

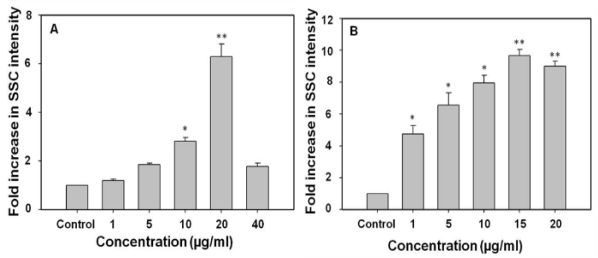

Fig. 1. Metal nanoparticles are significantly internalized in *D. radiodurans* cells as analyzed by flow cytometry. (A) AuNPs and (B) AgNPs uptake graphs were plotted as fold change in SSC intensity and thus uptake of nanomaterials in comparison to control. Data expressed as SE calculated from three (n=3) independent experiments. *p<0.05, ** p<0.01 compared to control.

Uptake and toxicity studies of metal NPs in D. radiodurans

D. radiodurans cells exhibited a pronounced concentration dependent increase in the uptake of AgNPs and AuNPs as indicated by an increase in the intensity of SSC. In case of AuNPs treatment, result showed the increase of 1.19, 1.84, 2.8, 6.29 and 1.7 fold at 1, 5, 10, 20 and 40 µg/mL concentration exposure respectively, when compared to the control cells (**Fig. 1A**). A statistically significant concentration dependent increase in the uptake was also observed in the SSC of *D. radiodurans* treated with different concentrations of AgNPs for 3 hrs (4.7, 6.5, 7.9, 9.6 and 8.9 fold at 1, 5, 10, 15 and 20 µg/mL concentration) (**Fig. 1B**). AuNPs and AgNPs showed significant increase in uptake frequency, up to 20 and 15 µg/mL concentration, respectively (**Fig. 1A** and **B**). At higher concentration, AuNPs internalization was decreased which could be due to the aggregation of AuNPs as evident by change of its color from purple to dark blue when suspended in buffer [32].

AgNPs showed better uptake than AuNPs, when similar concentration was exposed to cells. Up to 15 µg/mL concentration there is continuous increase in uptake, however, shows saturation at higher concentration than 20 µg/mL. Increased uptake can be

explained on the basis that AgNPs tends to induce membrane damage which facilitate the particle entry into the cells.

Toxicity and ROS generation due to metal NPs was also investigated simultaneously. Result showed that AgNPs are highly toxic for *D. radiodurans* and kill ~75% of total population (**Fig. 2B**), as also published by other researchers for different bacterial strains [1]. **Fig.2D** shows that AgNPs also causes significant increase in the ROS generation (~300%). Whereas, AuNPs are less toxic to *D. radiodurans* cells (**Fig. 2A**) which is also resulted in decreased ROS generation (**Fig. 2C**) up to the tested concentrations (20 µg/mL). AuNPs are reported to not have any significant effect on the growth of *E. coli* up to 100 µg/mL concentration [15], thus, considered as non-toxic or less toxic to the bacterial cells [33, 34]. Further, citrate AuNPs have a susceptibility to aggregate in the salt solution or media and hence aggregated particles are less prone to interact with in the cells [35]. Toxicity of AgNPs are apparently due to the solubilized Ag ions in the media [1]. Proteomic analysis reveals that AgNPs targets the bacterial cell membrane, leads to dissipation of proton motive force in *E. coli* due to substantial loss of intracellular potassium. AgNPs destabilizes the outer cell membrane and disrupt the barrier components such as lipopolysaccharide or porins, leading perturbation of the cytoplasmic membrane. AgNPs also reduces the cellular ATP level in *E. coli*, leading to collapse of membrane potential [14, 36].

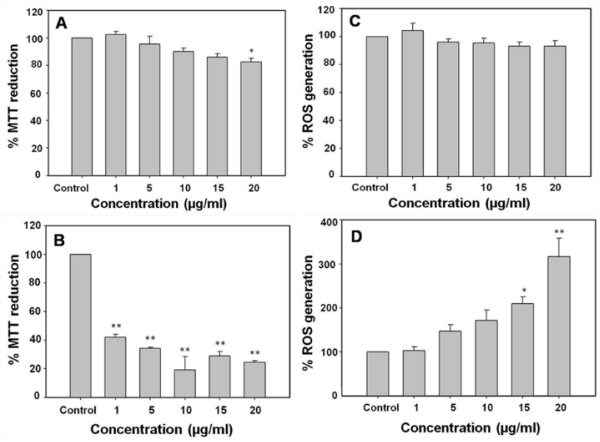

Fig. 2. Toxicity of metal nanoparticles to *D. radiodurans* cells were analyzed. Cell viability and ROS generation were estimated by MTT and DCFDA assay respectively. (A) and (B) simultaneously represent the % change in cell viability of bacterial cells after 3hrs exposure to AuNPs and AgNPs, (C) and (D) shows the % change in ROS generation by AuNPs and AgNPs exposure to bacterial cells, respectively. Data expressed as SE calculated from three (n=3) independent experiments. *p<0.05, ** p<0.01 compared to control.

Internalization and toxic effect of metal oxide NPs to D. radiodurans.

A significant uptake of NPs was observed in *D. radiodurans* cells treated with different concentrations of CuO and TiO_2 NPs as evident by an increase in the intensity of SSC after 3 hrs of exposure when compared with control. A statistically significant concentration dependent increase in the uptake was observed in the SSC of *D. radiodurans* cells treated with different concentrations (5, 10, 20, 40, 80 µg/mL) of CuO NPs which showed 2.17, 3.83, 8.00 10.3 and 11.9 increase in fold uptake than control (**Fig. 3A**).

Similarly, cells treated with different concentration of TiO_2 NPs as (6.7, 9.9, 13.9, 13.3 and 10.3-fold increase at 5, 10, 20, 40, 80 µg/mL concentrations) when compared to control (**Fig. 3B**). Uptake data suggests that both of these metal oxide particles actively internalized into the bacterial cells.

TiO_2 NPs (**Fig. 3B**) shows higher uptake than CuO NPs (**Fig. 3A**). It is also reported earlier by TEM and flow cytometry that TiO_2 NPs exhibit more internalization in *E. coli* cells in comparison to ZnO NPs [2].

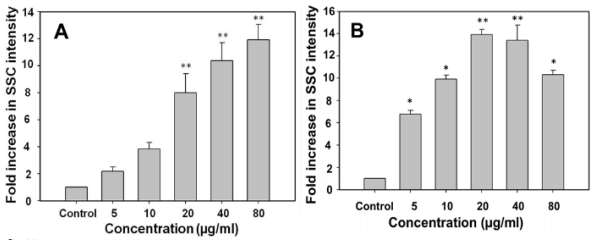

Fig. 3. Metal oxide nanoparticles are significantly internalized in *D. radiodurans* cells as analyzed by flow cytometry. (A) CuO, and (B) TiO_2, uptake graphs were plotted as fold change in SSC intensity and thus uptake of nanomaterials in comparison to control. Data expressed as SE calculated from three (n=3) independent experiments. *p<0.05, ** p<0.01 compared to control.

MTT studies of TiO_2 NPs revealed that these particles are non-toxic to *D. radiodurans* cells (**Fig. 4B**), which is corroborated by ROS results (**Fig. 4D**). Only at higher concentration of 40 and 80 µg/mL, TiO_2 NPs exhibited very less toxicity (~15-20%) and increased ROS generation (~120%). Whereas, exposure of CuO NPs reduces the cell's viability up to 50% (**Fig. 4A**) at same concentration and also induces the ROS generation up to 250% (**Fig. 4C**). It is reported that, metal oxide NPs can bind to the sulfur containing membrane/cellular proteins and also to macromolecules with phosphorous such as DNA which may lead to adverse effect on the cells [2]. Our result revealed that TiO_2 NPs are non-toxic to *D. radiodurans* cells which also agrees with previous observations that TiO_2 NPs does not exhibit toxic effect [17, 37] whereas, ROS generation was seen at very high concentration of 500 mg/L [3, 37]. Toxicity of CuO NPs was possibly due to the leaching of Cu ions in the culture medium [17]. Internalized NPs, are reported to inhibit the respiratory enzymes inside cells [2, 38] which leads to ROS production and thus damages the cellular lipids, carbohydrates, proteins and DNA and ultimately cell death [2, 18]. Several metal oxide NPs are shown to alter the microenvironment around the bacteria and produce ROS, which can induce bacterial damage. Therefore, the toxicity of oxide NPs (e.g., ZnO, CuO and TiO_2) does not always caused due to the NPs internalized into the bacteria [11, 17]. NPs can cause ROS generation by

different ways [39, 40], like they can induce spontaneous ROS generation at their surface because of their chemical and surface characteristics and interaction with cellular components or by activation of NADPH oxidase enzyme [7, 41]. Superoxide anion radicals and hydroxyl radicals are produced by the reaction of electrons and holes with oxygen and hydroxyl ions respectively, presented in the aqueous medium surrounding NPs. It has also been reported that the crystal defects caused due to oxygen vacancies leads to the production of large number of electron–hole pairs, which can migrate to the NPs surface and contribute to ROS generation [2, 42].

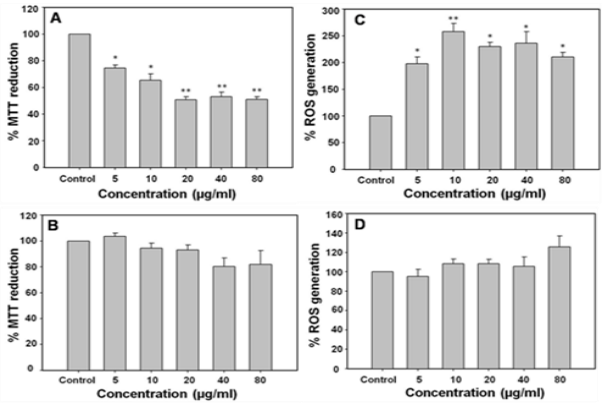

Fig. 4. Metal oxide nanoparticles are toxic to *D. radiodurans* cells. Cell viability and ROS generation were estimated by MTT and DCFDA assay respectively. (A) and (B) simultaneously represent the % change in cell viability of bacterial cells after 3hrs exposure to CuO and TiO_2. (C) and (D) shows the % change in ROS generation by CuO and TiO_2 exposure to bacterial cells, respectively. Data expressed as SE calculated from three (n=3) independent experiments. *p<0.05, ** p<0.01 compared to control.

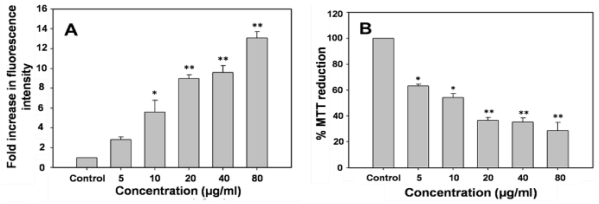

Fig. 5. (A) QDs nanoparticles are significantly internalized in *D. radiodurans* cells as analyzed by flow cytometry, graphs were plotted as fold change in SSC intensity and thus uptake of nanomaterials in comparison to control. (B) represent the % change in cell viability of bacterial cells after 3hrs exposure to QDs. Data expressed as SE calculated from three (n=3) independent experiments. *p<0.05, ** p<0.01 compared to control.

Interaction of D. radiodurans with CdTe QDs

QDs internalization was followed by its fluorescence intensity. Exposure of *D. radiodurans* cells to QDs resulted a pronounced increase in the uptake as indicated by an increase in the intensity of fluorescence of QDs as (2.8, 5.59, 8.96, 9.59 and 13.0-fold increase at 5, 10, 20, 40 and 80 µg/mL concentration, respectively) when compared to the control cells (**Fig. 5A**). QDs are reported to exhibit concentration dependent increase in fluorescence intensity which signifies the QDs internalization/adsorption in bacterial cells [43]. It is reported that CdSe QDs were internalized into bacterial cells through purine dependent mechanism in both gram positive and gram negative bacteria [44]. QDs can also be passively internalized in to the *P. aeruginosa* [43].

Toxicity study by MTT assay reveals that the QDs are also toxic to the *D. radiodurans* cells and causes decreases in cell viability up to 75% (**Fig. 5B**), but ROS generation experiment was not performed because both QDs and H_2DCFDA dye emits in same range. It has been reported earlier that toxicity of CdTe QDs was due to the release of Cd^{2+} ions into the media. They induces the expression of genes concerned with Cd^{2+} stress (ZntA and ZnuA). Tellurium is not thought to be the main reason of toxicity because cells incorporate it in very low amount. Further in aqueous solution, telluride (Te^{2-}) is oxidized to insoluble Te^0 [45]. Hence, the main toxicity of CdTe QDs is associated with Cd release, which extends oxidative stress and loss of membrane integrity. Upon interaction with membrane, QDs generates membrane stress condition and leads to modulation of several transporters (Omp F, Omp W) [19]. Cd^{2+} can easily enter to the cells through many divalent metal transporters [46] and interact with thiol groups. This condition generates oxidative stress due to depletion of intracellular thiol [47]. Intracellular ROS generation can lead to several types of damages, like protein oxidation and the release of Fe^{2+} from iron sulfur clusters [48].

Uptake and toxicity of Carbon based NMs GO, CNTs and fullerenes in D. radiodurans

A significant uptake of carbon based NMs (GO, CNTs and Fullerenes) was observed in *D. radiodurans* cells treated with different concentrations of these NMs (5, 10, 20, 40, 80 µg/mL). Bacterial cells show 5.2, 14.0, 23.5, 45.7, 59.0-fold increase in NMs uptake in comparison to control cells when exposed to different concentration of GO i.e. 5, 10, 20, 40 and 80 µg/mL concentration respectively. (**Fig. 6A**). Similar concentration dependent increase in the uptake was also observed in *D. radiodurans* cells exposed to CNTs. Data revealed that at 3 hrs exposure to different CNTs concentration (5, 10, 20, 40, 80 µg/mL) *D. radiodurans* cells showed 2.89, 8.86, 12.3, 20.15, 25.77-fold increase in SSC intensity with respect to control (**Fig. 6B**). Uptake and interaction of NMs to bacterial cells were examined by TEM and SEM imaging, respectively. TEM images clearly depicts that the GO and CNTs are internalized in bacterial cells and also causes morphological change from tetrad to diad form (**Fig. 8**). This is in agreement with the internalization result showed by flow cytometry. SEM analysis also showed that GO and CNTs exhibit significant interaction with the bacterial cells surface (Fig. ESI 1). Uptake studies of fullerenes by flow cytometry also showed a concentration dependent increase in uptake of 1.25, 1.56, 2.83, 4.48 fold in comparison to control cells at 5, 10, 20, 40, 80 µg/mL concentrations
(**Fig. 6C**).

Next, we have studied the cell viability and ROS generation events due to carbon NMs. MTT data shows that GO was toxic to bacterial cells as its exposure decreases the viability up to 50% when exposed to 40

µg/mL concentration (**Fig. 7A**). Result also revealed that there is significant increase (~550%) in intracellular ROS generation (**Fig. 7C**) upon exposure to 40 µg/mL GO concentration. MTT and ROS generation studies in fullerenes exposed bacterial cells showed that fullerenes do not exhibit significant toxic effect up to 40 µg/mL concentration (**Fig. 7B**) and also does not induces ROS generation in bacterial cells (**Fig. 7D**). Toxicity of GO nano sheets can be corresponding to its highest internalization in the bacterial cells. Antimicrobial activity of carbon nanostructures were reported earlier on both gram positive (*Staphylococcus aureus*) and gram negative (*E. coli*) bacterial cells [49, 50]. Among carbon nanostructures, fullerenes, SWCNTs and GO NMs and their derivatives were found to be more efficient as antibacterial agents.

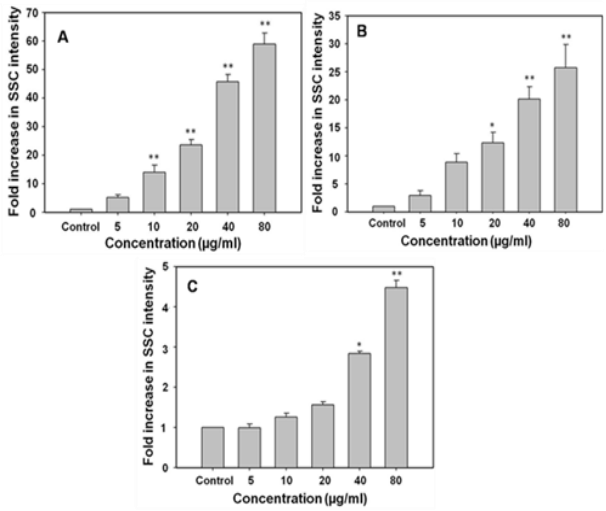

Fig. 6. Carbon based nanomaterials are significantly internalized in *D. radiodurans* cells as analyzed by flow cytometry. (A) GO, (B) CNTs and (C) Fullerenes uptake graphs were plotted as fold change in SSC intensity and thus uptake of nanomaterials in comparison to control. Data expressed as SE calculated from three (n=3) independent experiments. *p<0.05, ** p<0.01 compared to control.

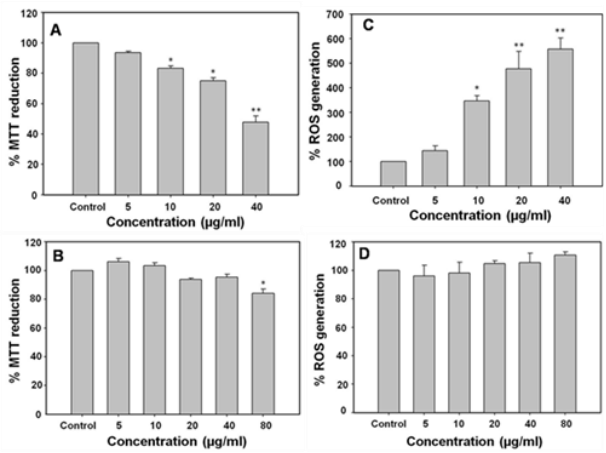

Fig. 7. Carbon based nanomaterials are toxic to *D. radiodurans* cells. Cell viability and ROS generation were estimated by MTT and DCFDA assay respectively. (A) and (B) simultaneously represent the % change in cell viability of bacterial cells after 3hrs exposure to GO and fullerenes. (C) and (D) shows the % change in ROS generation by GO and fullerenes exposure to bacterial cells, respectively. Data expressed as SE calculated from three (n=3) independent experiments. *p<0.05, ** p<0.01 compared to control.

Membrane stress caused due to physical interaction of GO sharp nano sheets with cells is the major cause of their antimicrobial property which may lead to RNA efflux [50-52]. Hydrogen bonding between specific outer cellular compartment and tetra pyrroles leads to the generation of intercellular hydroxyl radicals through aqueous leaching of Zn^{2+} which can be the main reason behind their antibacterial mechanisms [51]. Furthermore, the surface chemistry and metal toxicity of functionalized GO played a major role in antibacterial activity against *E. coli* [20, 51]. The less toxicity of fullerenes can be correlated with the lowest uptake. Fullerenes also showed no significant toxicity to human lung cancer cells (A549) as shown by TEM images of cellular structure and cell viability assays [53]. Toxicity studies of CNTs were not performed in this study, due to its interaction with the MTT dye [54]. But reports suggest that CNTs are known to damage the bacterial membrane, leading to the release of cytoplasmic elements [3, 55, 56].

Among all the tested NMs, carbon based NMs i.e. GO and CNTs shows the maximum internalization (**Fig. 6A** and **B**) in bacterial cells than metal, metal oxide and QDs. Fullerenes shows lowest internalization (**Fig. 6C**) which could be due to its bulky size. Toxicity of CNTs and GO could be due to physical interaction with cell membrane, formation of cell/CNTs/GO aggregates, or induction of cell membrane disruption [49, 57]. Whereas, toxicity of fullerenes are suggested due to the impairment of respiratory chain and inhibition of energy metabolism [20]. CNTs and GO NPs are reported to challenge the membrane integrity of bacterial cells, and therefore could be the reason that they get easily internalized. Highest internalization of carbon based NMs than other particles can be explained on the basis, that carbon is basic necessity for any organism to survive.

D. radiodurans also requires carbon for the growth and energy production [21], thus bacteria can sense the carbon based NMs as their nutrient source. In deinococcus, carbohydrates are imported through phosphoenolpyruvate phosphotransferase encoded on their mega plasmid [21, 58], so, there will be great possibility that carbon based NMs are also internalized through this route. On the other hand, its highest uptake result in flow cytometry can also be justified by the fact that the size of GO and CNTs are larger than all the particles tested, and thus it can lead to higher granularity (SSC).

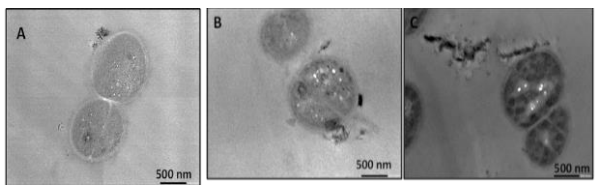

Fig. 8. TEM image shows that carbon based nanomaterials (GO and CNTs) shows interaction with *D. radiodurans* cells and get internalized. (A) Represent the control cells i.e. without any treatment, (C) and (D) shows the bacterial cells treated with 80 µg/ml GO and CNTs, respectively for 3 hrs.

Conclusion

Carbon based NMs can mimic the important carbon nutrients for *D. radiodurans*, thus can be easily internalize in to the bacterial cell through membrane transporters. Whereas, all other particles possess the same internalization level as depicted by SSC intensity. AgNPs are the most toxic among all of the above tested NMs and cause extensive ROS generation inside the cells, which is the main reason of cell death. Toxicity of AgNPs were thought to be mainly due to the leaching of Ag ions in media. AuNPs and TiO_2 NPs doesn't produce any ROS and thus are least toxic for the bacterial cells.

Acknowledgements

R. Singh thanks to Department of Science and Technology, New Delhi for providing INSPIRE Senior Research Fellowship (SRF). The financial assistance for the Centre for Nanotechnology Research and Applications (CENTRA) by The Gujarat Institute for Chemical Technology (GICT) is acknowledged.

References

1. O. Bondarenko, K. Juganson, A. Ivask, K. Kasemets, M. Mortimer, A. Kahru. Arch Toxicol. 87 (2013) 1181-1200.
2. A. Kumar, A. K. Pandey, S. S. Singh, R. Shanker, A. Dhawan. Free Radic Biol Med. 51 (2011) 1872-1881.
3. A. Simon-Deckers, S. Loo, M. Mayne-L'hermite, N. Herlin-Boime, N. Menguy, C. Reynaud, et al. Environ Sci Technol. 43 (2009) 8423-8429.
4. N. Kumar, V. Shah, V. K. Walker. J Hazard Mater. 190 (2011) 816-822.
5. M. A. Molina, J. L. Ramos, M. Espinosa-Urgel. Environ Microbiol. 8 (2006) 639-647.
6. S. C. Van Wees, S. Van der Ent, C. M. Pieterse. Curr Opin Plant Biol. 11 (2008) 443-448.
7. P. Gajjar, B. Pettee, D. W. Britt, W. Huang, W. P. Johnson, A. J. Anderson. J Biol Eng. 3 (2009) 9.
8. A. Thill, O. Zeyons, O. Spalla, F. Chauvat, J. Rose, M. Auffan, et al. Environ Sci Technol. 40 (2006) 6151-6156.
9. A. E. Nel, L. Madler, D. Velegol, T. Xia, E. M. Hoek, P. Somasundaran, et al. Nat Mater. 8 (2009) 543-557.
10. S. J. Soenen, P. Rivera-Gil, J.-M. Montenegro, W. J. Parak, S. C. De Smedt, K. Braeckmans. Nano Today. 6 (2011) 446-465.
11. M. J. Hajipour, K. M. Fromm, A. Akbar Ashkarran, D. Jimenez de Aberasturi, I. R. d. Larramendi, T. Rojo, et al. Trends in Biotechnology. 30 (2012) 499-511.
12. M. R. Brown, D. G. Allison, P. Gilbert. J Antimicrob Chemother. 22 (1988) 777-780.
13. T. F. Mah, G. A. O'Toole. Trends Microbiol. 9 (2001) 34-39.
14. C. N. Lok, C. M. Ho, R. Chen, Q. Y. He, W. Y. Yu, H. Sun, et al. J Proteome Res. 5 (2006) 916-924.
15. S. Chatterjee, A. Bandyopadhyay, K. Sarkar. J Nanobiotechnology. 9 (2011) 34.
16. E. E. Connor, J. Mwamuka, A. Gole, C. J. Murphy, M. D. Wyatt. Small. 1 (2005) 325-327.
17. M. Heinlaan, A. Ivask, I. Blinova, H. C. Dubourguier, A. Kahru. Chemosphere. 71 (2008) 1308-1316.
18. K. Kasemets, A. Ivask, H. C. Dubourguier, A. Kahru. Toxicol In Vitro. 23 (2009) 1116-1122.
19. J. P. Monras, B. Collao, R. C. Molina-Quiroz, G. A. Pradenas, L. A. Saona, V. Duran-Toro, et al. BMC Genomics. 15 (2014) 1099.
20. S. Maleki Dizaj, A. Mennati, S. Jafari, K. Khezri, K. Adibkia. Adv Pharm Bull. 5 (2015) 19-23.
21. D. Slade, M. Radman. Microbiol Mol Biol Rev. 75 (2011) 133-191.
22. N. Anaganti, B. Basu, A. Gupta, D. Joseph, S. K. Apte. Proteomics. 15 (2015) 89-97.
23. M. J. Daly, E. K. Gaidamakova, V. Y. Matrosova, J. G. Kiang, R. Fukumoto, D. Y. Lee, et al. PLoS One. 5 (2010) e12570.
24. P. Lancy, Jr., R. G. Murray. Can J Microbiol. 24 (1978) 162-176.
25. M. J. Thornley, R. W. Horne, A. M. Glauert. Archiv für Mikrobiologie. 51 (1965) 267-289.
26. R. Brayner, R. Ferrari-Iliou, N. Brivois, S. Djediat, M. F. Benedetti, F. Fievet. Nano Lett. 6 (2006) 866-870.
27. Z. Huang, X. Zheng, D. Yan, G. Yin, X. Liao, Y. Kang, et al. Langmuir. 24 (2008) 4140-4144.
28. K. H. Tam, A. B. Djurišić, C. M. N. Chan, Y. Y. Xi, C. W. Tse, Y. H. Leung, et al. Thin Solid Films. 516 (2008) 6167-6174.
29. A. Kumar, A. K. Pandey, S. S. Singh, R. Shanker, A. Dhawan. Chemosphere. 83 (2011) 1124-1132.
30. H. Suzuki, T. Toyooka, Y. Ibuki. Environ Sci Technol. 41 (2007) 3018-3024.
31. A. Xu, Y. Chai, T. Nohmi, T. K. Hei. Part Fibre Toxicol. 6 (2009) 3.
32. N. R. Tiwari, A. Rathore, A. Prabhune, S. K. Kulkarni. Advances in Bioscience and Biotechnology. Vol.01No.04 (2010) 8.
33. T. Chatterjee, S. Chakraborti, P. Joshi, S. P. Singh, V. Gupta, P. Chakrabarti. FEBS J. 277 (2010) 4184-4194.
34. J. Liu, C. Vipulanandan. Mater Sci Eng C Mater Biol Appl. 33 (2013) 3909-3915.
35. Makumire, Stanley. University of Zululand Institutional Repository. (2014)
36. W. Epstein. Prog Nucleic Acid Res Mol Biol. 75 (2003) 293-320.
37. L. K. Adams, D. Y. Lyon, P. J. Alvarez. Water Res. 40 (2006) 3527-3532.
38. S. Pal, Y. K. Tak, J. M. Song. Appl Environ Microbiol. 73 (2007) 1712-1720.
39. J. Song, H. Kong, J. Jang. Chem Commun (Camb). (2009) 5418-5420.
40. T. Xia, M. Kovochich, J. Brant, M. Hotze, J. Sempf, T. Oberley, et al. Nano Lett. 6 (2006) 1794-1807.
41. T. Xia, M. Kovochich, M. Liong, L. Madler, B. Gilbert, H. Shi, et al. ACS Nano. 2 (2008) 2121-2134.
42. J. W. Rasmussen, E. Martinez, P. Louka, D. G. Wingett. Expert Opin Drug Deliv. 7 (2010) 1063-1077.
43. Chen T., Hongyan Ma, Kristy Katzenmeyer, J. D. Bryers. Journal of Undergraduate Research in Bioengineering.
44. J. A. Kloepfer, R. E. Mielke, J. L. Nadeau. Appl Environ Microbiol. 71 (2005) 2548-2557.
45. T. G. Chasteen, D. E. Fuentes, J. C. Tantalean, C. C. Vasquez. FEMS Microbiol Rev. 33 (2009) 820-832.
46. H. Makui, E. Roig, S. T. Cole, J. D. Helmann, P. Gros, M. F. Cellier. Mol Microbiol. 35 (2000) 1065-1078.
47. A. Wang, D. E. Crowley. J Bacteriol. 187 (2005) 3259-3266.
48. J. A. Imlay. Annu Rev Microbiol. 57 (2003) 395-418.
49. Z. Lu, T. Dai, L. Huang, D. B. Kurup, G. P. Tegos, A. Jahnke, et al. Nanomedicine (Lond). 5 (2010) 1525-1533.
50. O. Akhavan, E. Ghaderi. ACS Nano. 4 (2010) 5731-5736.
51. S. Azimi, J. Behin, R. Abiri, L. Rajabi, A. A. Derakhshan, H. Karimnezhad. Science of Advanced Materials. 6 (2014) 771-781.
52. S. Gurunathan, J. W. Han, A. A. Dayem, V. Eppakayala, J. H. Kim. Int J Nanomedicine. 7 (2012) 5901-5914.
53. F. Wang, C. Jin, H. Liang, Y. Tang, H. Zhang, Y. Yang. Environmental Toxicology and Pharmacology. 37 (2014) 656-661.
54. L. Belyanskaya, P. Manser, P. Spohn, A. Bruinink, P. Wick. Carbon. 45 (2007) 2643-2648.
55. S. Kang, M. S. Mauter, M. Elimelech. Environ Sci Technol., 42 (2008) 7528-7534.
56. S. Kang, M. Herzberg, D. F. Rodrigues, M. Elimelech. Langmuir. 24 (2008) 6409-6413.
57. S. Kang, M. Pinault, L. D. Pfefferle, M. Elimelech. Langmuir. 23 (2007) 8670-8673.
58. O. White, J. A. Eisen, J. F. Heidelberg, E. K. Hickey, J. D. Peterson, R. J. Dodson, et al. Science. 286 (1999) 1571-1577.

